Defect generation by preferred nucleation in epitaxial Sr_2RuO_4/$LaAlO_3$

Mark A. Zurbuchen,[a] Yunfa Jia, Stacy Knapp, Altaf H. Carim,[b] and Darrell G. Schlom
Department of Materials Science and Engineering, The Pennsylvania State University,
University Park, Pennsylvania 16803-6602

X. Q. Pan
Department of Materials Science and Engineering, University of Michigan, Ann Arbor,
Michigan 48109-2136

The atomic structure of the film–substrate interface of a (001) Sr_2RuO_4/(100)$_c$ $LaAlO_3$ film, determined by high-resolution transmission electron microscopy and simulation, is reported. The structure of superconductivity-quenching $\Delta c \approx 0.25$ nm out-of-phase boundaries (OPBs) in the film is also reported. Growth in one region on the La-terminated surface is observed to nucleate with a SrO layer. Because two structurally equivalent SrO layers exist within the unit cell, two neighboring nuclei with differing growth order (SrO-RuO_2-SrO or RuO_2-SrO-SrO) will nucleate an OPB where their misaligned growth fronts meet. Strategies to avoid OPB generation by this mechanism are suggested, which it is hoped may ultimately lead to superconducting Sr_2RuO_4 films. © *2003 American Institute of Physics.*
[DOI: 10.1063/1.1624631]

Sr_2RuO_4 is the only known copper-free layered perovskite superconductor,[1] and is believed to have an unconventional spin-triplet (p-wave) symmetry of the superconducting order parameter.[2] Electrical transport studies of Sr_2RuO_4 are expected to further the understanding of the superconducting state.[3] Sr_2RuO_4 is well lattice-matched to $YBa_2Cu_3O_{7-\delta}$ and other cuprate superconductors. Epitaxial heterostructures would be useful for probing the interaction between d-wave and p-wave superconductors. Although the epitaxial growth of Sr_2RuO_4 films[4,5] and epitaxial $YBa_2Cu_3O_{7-\delta}$/Sr_2RuO_4 heterostructures[6] have been demonstrated, no superconducting Sr_2RuO_4 films have been reported.[4,5] As we show in this letter, greater attention to nucleation and growth is important to reducing defects and to possibly achieving superconductivity in Sr_2RuO_4 films.

Both impurities and crystallographic defects can quench superconductivity in Sr_2RuO_4. As little as 300 ppm of aluminum is sufficient to destroy superconductivity.[7] Crystallographic defects that quench superconductivity include out-of-phase boundaries (OPBs).[8] These are translation boundaries consisting of a fractional misalignment in the long axis (c-axis) direction between two neighboring regions of the same crystal. Because any interruption of the structure can act as a pair-breaker, a linear density of OPBs on the order of $1/\xi_{ab}(0)$, where $\xi_{ab}(0)$ is the superconducting coherence length in the (001) plane, $\xi_{ab}(0) \approx 66$ nm,[9] renders a high-purity film nonsuperconducting.[9] A correlation between T_c and the residual resistivity (ρ_0), a measure of disorder in equivalent-purity crystals, has also been reported.[10] Although OPBs are common defects in complex oxides, little is known about their nucleation mechanisms or impact upon properties.[11–13]

In the heteroepitaxial growth of layered structures, substrate surface quality has a great effect on final film quality.[14] Advances in substrate engineering have enabled the preparation of substrates with known atomic terminations.[14,15] Some disagreement currently exists regarding the atomic termination of (001) $LaAlO_3$.[16–19]

It would be useful experimentally to determine which atomic layers are energetically preferred for the nucleation of Sr_2RuO_4 on a given substrate, so that high-quality films can be grown by sequential deposition techniques [e.g., molecular-beam epitaxy (MBE)]. Few studies of the preferred nucleation layer of epitaxial thin films of complex oxides on substrates with known termination have been reported.[20–22] Understanding defect nucleation mechanisms and microstructural development in the growth of complex oxide films will allow greater control over their growth. Substrate surface features have been demonstrated to result in micron-scale crystallographic defects in some similarly structured layered perovskites ($n = 2$ Aurivillius phases).[23,24] In this letter, the structure of the film–substrate interface of an epitaxial (001) Sr_2RuO_4/(001)$_c$ $LaAlO_3$[16] film is reported, and the mechanism whereby the preferred nucleation layer can lead to the generation of superconductivity-quenching OPBs is described.

(001)$_c$ Sr_2RuO_4 epitaxial films were grown on (001) $LaAlO_3$[16] substrates by pulsed-laser deposition (PLD) at 1000 °C in a radiatively heated sample chamber. Specifics of the film growth are described in detail elsewhere.[8] The film described here was a high-quality film, judged by the full width at half-maximum of the 006 Sr_2RuO_4 peak of approximately 0.23° in 2θ, and 0.33° in ω (instrumental resolution $\approx 0.20°$) in x-ray diffraction measurements. Samples for cross-sectional transmission electron microscopy (TEM) examination were prepared by standard sandwiching, slicing, dimpling, and argon ion milling on a liquid nitrogen-cooled stage at 4 kV and 8° to 11°.

---

[a]Presently at: Argonne National Laboratory, Argonne, IL; electronic mail: mark_z@mac.com
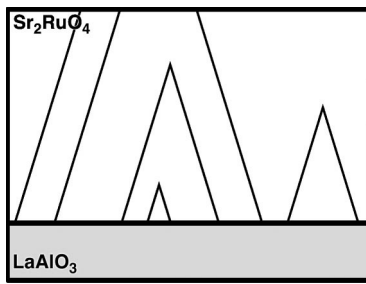[b]Presently at: the U.S. Department of Energy, Germantown, MD.

FIG. 1. Schematic of the planar defect morphology of OPBs in $SrRu_2O_4$/$LaAlO_3$ films; diagonal lines represent OPBs. Two OPBs with opposing inclination, on the far right, have annihilated where they met. On the far left, two OPBs with parallel inclination penetrate through the full thickness of the film.

High-resolution TEM (HRTEM) imaging was performed using JEOL 4000-EX and Hitachi HF-2000 microscopes. Regions of appropriate and consistent thickness of the film–substrate phase boundary and an individual OPB were located, and through-focus image series were acquired. Appropriate multislice simulation parameters were determined by matching of images to simulated images of the individual phases, and supercells based on possible interfacial and defect structures were constructed. HRTEM image simulations used sufficiently large supercells to remove cell-edge distortions, caused by their nonrepeating nature, from the region of interest. Bulk values for a and b of Sr_2RuO_4 and $LaAlO_3$ were used in constructing the interfacial models, with cells aligned in the center. The 2.1% lattice mismatch between $(001)_c$ $LaAlO_3$[16] and (001) Sr_2RuO_4 at room temperature resulted in negligible variation in alignment (0.12 Å) over the length scale of the supercell. As a check, simulations of a coherent interface were also performed, with identical results. Only the 2.1% lattice-mismatched supercell simulations are presented here.

Figure 1 shows a schematic of the generalized defect morphology we have observed in (001) Sr_2RuO_4/$(001)_c$ $LaAlO_3$[16] epitaxial films.[8,23] Films contain a number of $\Delta c \approx 0.25$ nm ($\sim c/5$) OPBs, inclined 17° from the c direction. These features either penetrate the full film thickness, or else annihilate where pairs of opposite inclination meet. Similar features in other $n=1$ Ruddlesden-Popper (RP)[25] phases have been reported,[11,12] although no detailed information on their structure or nucleation is available.

A [100] HRTEM image of a single OPB, showing a (011) habit, is shown in Fig. 2. A model and HRTEM simulation are inset, showing a very good match with the image. Both chemical and physical interruptions of the structure exist at the OPB. A distorted rocksalt SrO layer is incorporated along the OPB. This lattice interruption not only will scatter phonons,[8] but also interrupts the continuity of the $a-b$ plane RuO_2 layers, believed to be responsible for superconductivity in the material.

Figure 3(a) shows a [100] HRTEM image of the film–substrate interface, with a Fourier-filtered region of the image on the right. Bright spots correspond to atomic columns. Models and HRTEM simulations for each of the possible termination-nucleation layer pairs are shown in Figs. 3(b)–3(f), with the exception of growth beginning with RuO_2 on an AlO_2-terminated surface, which was ruled out because no known phases with the corresponding structure could be
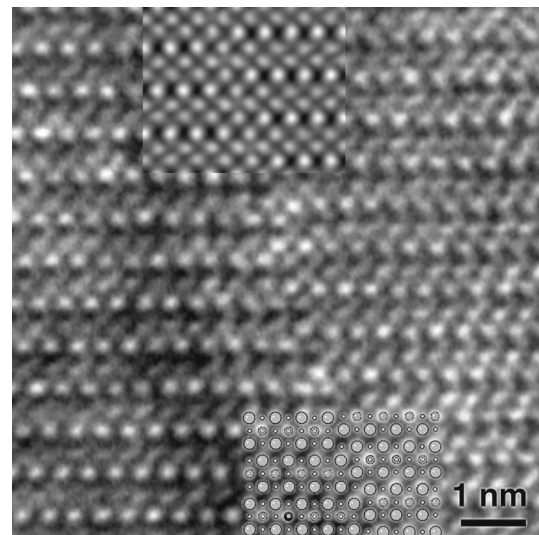

FIG. 2. HRTEM image of a single OPB in a (001) $SrRu_2O_4$/$(001)_c$ $LaAlO_3$ film, with a model and simulation of the defect inset. Large circles represent strontium, small circles ruthenium. An extra SrO layer is incorporated along the OPB. The c-direction misregistry across the OPB is 0.25 nm, equal to the c-direction dimension of a single layer of SrO.

found. Close examination of the images reveals that only the model in Fig. 3(d), with a charge-neutral SrO layer nucleating on a LaO-terminated surface, matches the HRTEM image. This result is consistent with the previous determination of a LaO surface termination of $LaAlO_3$ above $\approx 300\,°C$ in vacuum or near vacuum.[17,19] Growth proceeds with a SrO-RuO_2-SrO layer ordering. The Sr_2RuO_4 unit cell contains two structurally equivalent SrO layers, and only one RuO_2 layer, and the OPB offset is equivalent to one SrO layer. There are, then, two possibilities for the nucleation mechanism. (i) If SrO is strongly energetically preferred as the starting layers, then a LaO-SrO-SrO-RuO_2 growth order, as shown in Fig. 3(c), might also be possible. However, this layer order contains three AO (rocksalt)-type layers in a row, which has never been observed in these RP nor in substoichiometric perovskite type phases,[26] so that it is considered to be unlikely. (ii) If the energy difference of a SrO versus a RuO_2 nucleation layer is small, then a LaO-RuO_2-SrO-SrO
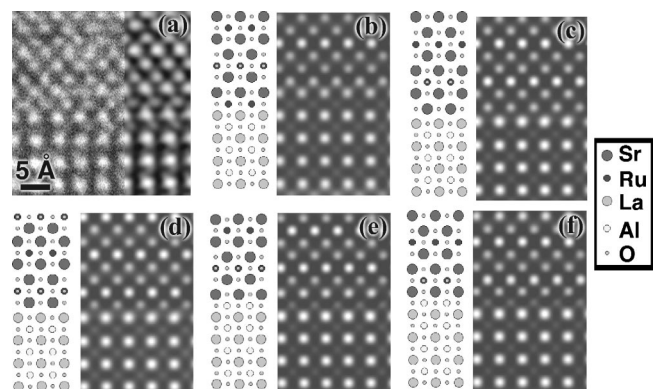

FIG. 3. (a) HRTEM image of the (001) Sr_2RuO_4/$(001)_c$ $LaAlO_3$ (see Ref. 16) film–substrate interface, taken at Scherzer defocus. A Fourier-filtered region of the image is overlaid on the right. (b)–(f) Models of the possible termination-nucleation layer pairs for the film, shown with HRTEM simulations ($\Delta f = -58$ nm, $t = 4.5$ nm). The model in (d) shows the only reasonable match with the image. The film nucleated with a SrO-RuO_2-SrO layer sequence on a LaO-terminated substrate.
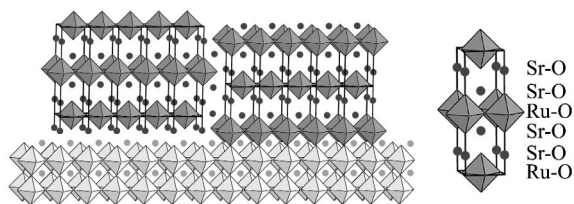
FIG. 4. Nucleation-layer growth-order OPB nucleation mechanism in the $(001) \, Sr_2RuO_4/(001)_c$ LaAlO$_3$ (see Ref. 16) film. Because two structurally equivalent SrO layers exist in the Sr_2RuO_4 unit cell, adjacent nuclei growing with either SrO-RuO$_2$-SrO or RuO$_2$-SrO-SrO ordering, will form an OPB where they meet. The coordination octahedra of the ruthenium and aluminum are shown, with circles representing strontium and lanthanum, in shades of gray equivalent to those in Fig. 3. A unit cell of Sr_2RuO_4 is shown to the right for reference.

growth order, as shown in Fig. 3(b), might also be possible. A schematic of this OPB nucleation mechanism, considered most likely to be correct, is shown in Fig. 4.

Growth proceeding in either of these scenarios would result in the generation of OPBs through the preferred nucleation mechanism. The energetics of continuing growth after the first layer would be expected to be quite similar, considering the close lattice match and the fact that each layer is charge neutral, so electrostatic effects do not affect growth ordering, as they undoubtedly do in other layered perovskites such as the Aurivillius phases. The c-direction misregistry of the OPBs is equal to the c dimension of a single SrO layer (i.e., an extra one or a missing one) within the unit cell. This implies that OPBs nucleated at the film–substrate interface (almost all of the OPBs observed) by the meeting of two nuclei with differing growth order.

Bearing this model in mind, we reconsider the general OPB morphology depicted in Fig. 1. Because neighboring out-of-phase nuclei have only one possible offset, OPB interaction is uncomplicated. Two OPBs with opposing inclinations, like those shown on the right in Fig. 1, will annihilate when the film growth front proceeds past the point where they meet. Two nuclei with parallel inclinations, like those shown on the left, will not interact and will penetrate the full film thickness.

Additional mechanisms that may also lead to the generation of OPBs in $n=1$ RP phases on perovskite substrates are surface steps,[23] and perhaps in the case of films on LaAlO$_3$ substrates, twinning of the substrate upon transformation during cooling from the growth temperature.[16] The slight tilt between domains could conceivably be accommodated by a defect having a similar appearance to the OPBs described here, although the linear OPB density in the samples we have examined ($\geqslant$1 of every 17 perovskite cells)[8] is much greater than the linear density of domain boundaries in LaAlO$_3$ is likely to be.

Several strategies that might suppress the nucleation-layer OPB generation mechanism in Sr_2RuO_4 films are possible, and could lead to lower OPB densities and possibly to the first superconducting Sr_2RuO_4 films. An atomic layer-by-layer growth technique such as MBE[27] could be used to engineer the growth order, for example, beginning growth with either the preferred SrO layer, or perhaps a RuO$_2$ layer, on a LaO-terminated substrate, and continuing with either sequence. Perhaps the best strategy would be to use a (001) LaSrAlO$_4$ substrate instead of $(001)_c$ LaAlO$_3$,[16] as LaSrAlO$_4$ is isostructural to Sr_2RuO_4. Lastly, extra kinetic activation (e.g., higher temperature, higher laser fluence) during growth of the first few atomic layers could increase surface diffusivities, increasing the average nuclei diameter,[28] thereby reducing the density of OPBs.

[1] Y. Maeno, H. Hashimoto, K. Yoshida, S. Nishizaki, T. Fujita, J. J. Bednorz, and F. Lichtenberg, Nature (London) **372**, 532 (1994).
[2] T. M. Rice and M. Sigrist, J. Phys. C **7**, L643 (1995).
[3] Y. Maeno, T. M. Rice, and M. Sigrist, Phys. Today **54**, 42 (2001).
[4] D. G. Schlom, Y. Jia, L.-N. Zou, J. H. Haeni, S. Briczinski, M. A. Zurbuchen, C. W. Leitz, S. Madhavan, S. Wozniak, Y. Liu, M. E. Hawley, G. W. Brown, A. Dabkowski, H. A. Dabkowska, R. Uecker, and P. Reiche, Proc. SPIE **3481**, 226 (1998).
[5] S. Ohashi, M. Lippmaa, N. Nakagawa, H. Nagasawa, H. Koinuma, and M. Kawasaki, Rev. Sci. Instrum. **70**, 178 (1999).
[6] F. Lichtenberg, A. Catana, J. Mannhart, and D. G. Schlom, Appl. Phys. Lett. **60**, 1138 (1992).
[7] A. P. Mackenzie, R. K. W. Haselwimmer, A. W. Tyler, G. G. Lonzarich, Y. Mori, S. Nishizaki, and Y. Maeno, Phys. Rev. Lett. **80**, 161 (1998).
[8] M. A. Zurbuchen, Y. Jia, S. K. Knapp, A. H. Carim, D. G. Schlom, L.-N. Zou, and Y. Liu, Appl. Phys. Lett. **78**, 2351 (2001).
[9] T. Akima, S. Nishizaki, and Y. Maeno, J. Phys. Soc. Jpn. **68**, 694 (1999).
[10] Z. Q. Mao, Y. Mori, and Y. Maeno, Phys. Rev. B **60**, 610 (1999).
[11] J. G. Wen, C. Traeholt, and H. W. Zandbergen, Physica C **205**, 354 (1993).
[12] G. Kong, M. O. Jones, J. S. Abell, P. P. Edwards, S. T. Lees, K. E. Gibbons, I. Gameson, and M. Aindow, J. Mater. Res. **16**, 3309 (2001).
[13] M. A. Zurbuchen, J. Lettieri, Y. Jia, D. G. Schlom, S. K. Streiffer, and M. E. Hawley, J. Mater. Res. **16**, 489 (2001).
[14] M. Kawasaki, K. Takahashi, T. Maeda, R. Tsuchiya, M. Shinohara, O. Ishiyama, T. Yonezawa, M. Yoshimoto, and H. Koinuma, Science **266**, 1540 (1994).
[15] T. Ohnishi, K. Takahashi, M. Nakamura, M. Kawasaki, M. Yoshimoto, and H. Koinuma, Appl. Phys. Lett. **74**, 2531 (1999).
[16] Cubic indices; LaAlO$_3$ is cubic at the film growth temperature, and transforms to rhombohedral on cooling.
[17] J.-P. Jacobs, M. A. San Miguel, and L. J. Alvarez, J. Mol. Struct.: THEOCHEM **390**, 193 (1997).
[18] D.-W. Kim, D.-H. Kim, B.-S. Kang, T. W. Noh, D. R. Lee, and K.-B. Lee, Appl. Phys. Lett. **74**, 2176 (1999).
[19] P. A. W. van der Heide and J. W. Rabalais, Chem. Phys. Lett. **297**, 350 (1998).
[20] S. Bals, G. Rijnders, D. H. A. Blank, and G. Van Tendeloo, Physica C **355**, 225 (2001).
[21] J. C. Jiang and X. Q. Pan, J. Appl. Phys. **89**, 6365 (2001).
[22] M. Salluzzo, C. Aruta, I. Maggio-Aprile, Ø. Fischer, S. Gals, and J. Zegenhagen, Phys. Status Solidi A **186**, 339 (2001).
[23] M. A. Zurbuchen, J. Lettieri, G. Asayama, Y. Jia, A. H. Carim, D. G. Schlom, and S. K. Streiffer (unpublished).
[24] B. Aurivillius, Ark. Kemi **1**, 463 (1950); **1**, 499 (1950); **2**, 519 (1951); **5**, 39 (1953).
[25] S. N. Ruddlesden and P. Popper, Acta Crystallogr. **10**, 538 (1957); **11**, 54 (1958).
[26] C. N. R. Rao and B. Raveau, *Transition Metal Oxides: Structure, Properties, and Synthesis of Ceramic Oxides*, 2nd ed. (Wiley, New York, 1998), p. 61.
[27] D. G. Schlom, J. H. Haeni, J. Lettieri, C. D. Theis, W. Tian, J. C. Jiang, and X. Q. Pan, Mater. Sci. Eng., B **87**, 282 (2001).
[28] B. Dam and B. Stäuble-Pümpin, J. Mater. Sci.: Mater. Electron. **9**, 217 (1998).